Regime Shift Models for Simulation of the Interaction between Benthic and Pelagic Production

Jan Kloppenborg Møller[1,2], Jacob Carstensen[2], Henrik Madsen[1]
[1] Informatics and Mathematical Modelling - DTU
[2] National Environmental Research Institute - NERI
IMM-Technical Report-2006-23

March 19, 2007

Contents

Chapter 1

Introduction

Eutrophication is a result of nutrient enrichment of ecosystems. For aquatic ecosystems the link between algae blooms and eutrophication was recognized in the 1960s (see Schindler (2006)). The main sources of eutrophication are nitrogen (N) and phosphorus (P), the human sources of these are industry and households (dominant source of P), and agriculture (dominant source of N).

In more recent years the hypothesis of alternative stable states have been proposed (see Schindler (2006), for a historic presentation). The presence of alternative stable states is potentially reflected in hysteresis effects and even irreversible changes of a system caused by excessive nutrient loading (eutrophication) on the system. There is a bulk literature on this subject in the context of lakes, e.g. Scheffer et al (2003), Carpenter (2005), and others. These kind of shifts where the dynamics of the system change suddenly will be referred to as regime shifts.

An example of a simple system with regime shifts is given in Carpenter et al (1999), here P in the water column is modeled as a function of the loadings. The dynamic equation include a non-linear recycling term. This construction give rise to alternative stable states and with the right choice of parameter values both hysteresis effects and irreversible changes.

Others (e.g. Scheffer et al (2003)) give examples of two dimensional (e.g. floating and submerged plants) systems with bistable dynamics. Scheffer et al (2003) offer a conceptual empirical verification of the bistable hypothesis in controlled experiments. Such verification are however difficult in real life systems. The presence of different time constants in the system may (as pointed out by Carpenter (2005)) appear to be hysteresis effect or even irreversible changes of the system, simply because the system may use hundreds or even thousands of years to recover after heavy loading coursing a break down of the system in a matter of years or decades. It could of course also be argued that the system from a practical

1

point of view has experienced an irreversible change.

An important issue for systems with alternative stable states is the stability of the states, such analysis can be addressed with bifurcation analysis (see e.g. Scheffer et al (2003)), and this will show how far the system is from an abrupt change. Since ecosystems are very complex systems there are bound to be noise in the systems ("systems noise"). On top of this measurements of these systems are bound to be uncertain. An adequate description of these systems is therefore a stochastic one. The stochastic nature of the system means that we can only assign a probability of a regime shift appearing in the next time interval, and it might therefore be the best strategy to use a precautionary policy.

Ludwig et al (2003) and Carpenter et al (1999) advocate for this point. These papers explore management strategies for lakes, by using an economic utility model on the top of the dynamical system description. Both papers advocate for a precautionary policy due to the uncertainty in the system. Ludwig et al (2003) have built a noise term into the model.

We will explore some models for the relation between the pelagic and benthic vegetation in marine ecosystems. The models are derived in a discrete time setting and not, as is often the case, derived from differential equation. We will present some characteristics of these system and emphasize where care is needed in order to ensure stability. The models are explored both in a deterministic setting and in a stochastic setting.

Chapter 2

A Benthic/Pelagic Interaction Model

2.1 The Concept

The conceptual setting is an ecosystem as sketch in Figure 2.1. The model has two states or regimes corresponding to high and low nutrient loading. In the first regime the ecosystem is in a "healthy" condition. I.e. the water is relatively clear, such that sun light is able to reach the benthic zone. In this regime there is a high level of benthic biomass and the sediment is therefore capable of permanently removing most of the nutrients in the particulate matter reaching the bottom, through denitrification.

The second regime is characterized by high level of pelagic biomass. This prevents sunlight from reaching the benthic zone and benthic vegetation will therefore be reduced or completely disappear. One result thereof is that the sediment becomes more susceptible to releasing nutrients back into the water column causing a further increase in phytoplankton biomass. The last effect is illustrated in Figure 2.1 with the double arrow.

Nutrient input is the driver of the system, but the benthic vegetation will govern the regimes. The figure indicates that the interaction goes through the sediment. This is also true on the conceptual level, but the sediment will be ignored in the first models. The ecosystem functioning will therefore be modeled directly as a interaction between benthic and pelagic production.

Sketch of a Marine Ecosystem

"Regime"   I   II

↓ Light

| Nutrient input low → | Phytoplankton level X_p Low | | Nutrient input high → | Phytoplankton level X_p High |

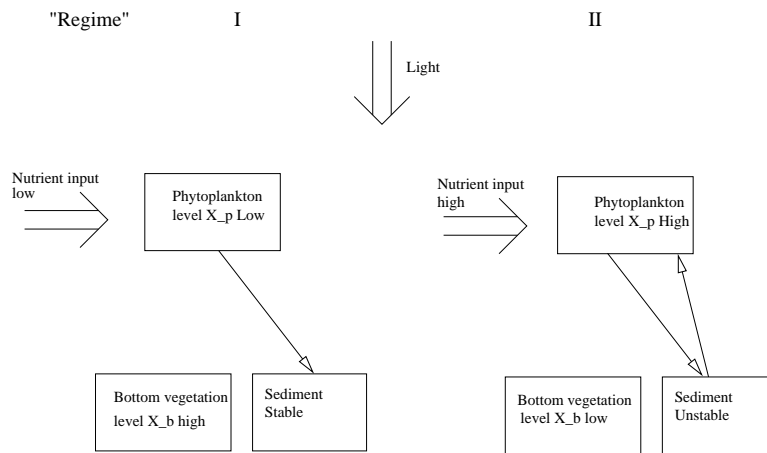| Bottom vegetation level X_b high | Sediment Stable | | Bottom vegetation level X_b low | Sediment Unstable |

Figure 2.1: Schematic picture of the model described in (2.1) and (2.2). Regime I is the healthy ecosystem where most of the nutrient from the phytoplankton is processed by the sediment through uptake and permanent burial. The sediment becomes overloaded in regime II causing faster cycling of the nutrients from the sediment, this is an "unhealthy" situation where benthos potentially may suffer from oxygen depletion.

4

2.2 A Hard Threshold Set Up

The conceptual setting described in Section 2.1 is now translated into a mathematical model. In the formulation given here units are arbitrary; the aim is here to describe the functional relationship. The proposed model is

$$X_{p,t} = a_p^{(j)} N_{ex,t} + b_f^{(j)} X_{p,t-1} + \epsilon_{p,t}^{(j)} \qquad (2.1)$$

$$X_{b,t} = (k^{(j)} + b_{p,b}^{(j)} X_{p,t-1}) f^{(j)}(X_{p,t-1}) + b_b^{(j)} X_{b,t-1} + \epsilon_{b,t}^{(j)} \qquad (2.2)$$

where

$$j = \begin{cases} 1 & \text{if } X_{b,t-1} > r_b \\ 2 & \text{if } X_{b,t-1} \leq r_b \end{cases} \qquad (2.3)$$

The formulation above is a bivariate nonlinear threshold model. The behavior of this model will be explored with simulation studies, but first each of the parameters/functions in the model will be presented with a physical/biological interpretation.

$\underline{X_{p,t} \text{ and } X_{b,t}}$**:**

The benthic biomass ($X_{b,t}$) of the ecosystem at time t and the pelagic biomass ($X_{p,t}$) at time t. These are the state variables of the system.

$\underline{N_{ex,t}}$**:**

The external nutrient loading on the system at time t.

$\underline{a_p^{(j)}}$**:**

The effect of nutrient loading on the system. This is a linear relationship (in each regime). Further it is seen that nutrient loading affects the phytoplankton level directly while it only affects the benthic vegetation level indirectly, through the effect of increased concentration of phytoplankton in the water column. If the state variables are considered as content of nutrients in the pelagic/benthic biomass, then $a_f^{(j)}$ could be viewed as a proportion.

$\underline{b_p^{(j)} \text{ and } b_b^{(j)}}$**:**

These parameters describe how much of the benthic and pelagic biomass that survive from year to year. These number are fractions, i.e. they should be between 0 and 1.

$\underline{f^{(j)}(x)}$**:**

$f^{(j)}(x)$ describes the effect on the benthic zone from increased level of phytoplankton in the pelagic zone. Increased level of pelagic biomass prevent sunlight from reaching the benthic zone, and this should be reflected in $f(x)$. $f^{(j)}(x)$ should therefore be close to one for low level of phytoplankton and close to zero for high level of phytoplankton, i.e. a sigmoid function. Here f is chosen as $f = 1 - \Phi(x)$ where Φ is the distribution function for the normal distribution. The behavior of this function is controlled by the mean and the variance in the normal distribution.

The function f should be written as

$$f^{(j)}(x) = f(x; r_p^{(j)}, \tau_p^{(j)}) = 1 - \Phi\left(x; r_p^{(j)}, \left(\tau_p^{(j)}\right)^2\right) \tag{2.4}$$

where r_p is a translation of the function such that $f(r_p) = \frac{1}{2}$, and τ_p controls how fast the changes in f is introduces, e.g. $f(r_p - 2\tau_p) \approx 0.95$, $f(r_p + 2\tau_p) \approx 0.05$.

$\underline{b_{p,b}^{(j)}}$**:**

A cross correlation term that describes the effect of nutrient carried from the pelagic zone to the benthic zone. This is in it self a linear relation, but it is damped by the nonlinear function f described above.

$\underline{k^{(j)}}$**:**

k describes a level of bottom vegetation, this is also damped by the nonlinear function f.

$\underline{r_b}$**:**

r_b is a threshold for the system, this construction allows dynamics of the system to change completely and instantaneously when the threshold is crossed, i.e. when x_b becomes less than r_b.

$\underline{\epsilon_{i,t}^{(j)}}$**:**

$\epsilon_{i,t}^{(j)}$ describes the errors at each time step; these should follow some probability distribution.

Remarks:

The model described by Eq. (2.1)-(2.3) is a nonlinear multivariate model with an input that drives the system. Univariate models with threshold parameters like r_b are called SETAR (Self Exiting Threshold Auto-Regressive) models, while univariate models with a nonlinear dampening term like f is called STAR (Smooth Threshold Auto-Regressive) models. There are other regime models that should be thought of, an example is hidden Markov models with regime switching.

The only difference between the regimes in the following studies will be in b_p ($b_p^{(1)} < b_p^{(2)}$), this means that X_p grows fast towards a new equilibrium when the regime shift occur. This in turn will have a catastrophic impact on the benthic vegetation.

In regime "I" where the sediment is stable, $b_p^{(j)}$ will be low since most of the biomass will be absorbed by the sediment. In regime "II" most of the nutrient which reach the bottom will be cycled to the water column.

The asymptotic mean value $x_p = \lim_{t\to\infty} E(X_{p,t})$ is $\frac{a_p^{(j)} N_{ex}}{1-b_p^{(j)}}$ under the assumption that the system will settle in one state and that the loading N remains constant. This means that x_p will be zero if N_{ex} is zero or if a_p is zero.

The first term in Eq. (2.2) describes how the phytoplankton level affects the benthic vegetation. For small values of $X_{p,t}$ compared to r_p (see Eq. (2.4)) the effect of a small change in X_p will be positive, i.e. the nutrient from the phytoplankton will be used by the benthic vegetation and increase the amount of benthic biomass. As $X_{p,t}$ becomes closer to r_p the shadow effect will be dominant and the first term in Eq. (2.2) will vanish, which results in a fast decay of X_b. When X_b crosses the threshold r_b a further rise in the X_p will cause the first term to decrease faster and X_b will approach zero.

The situation above should reflect the situation in a marine ecosystem as a rise in the level of phytoplankton cause the benthic vegetation to shaded out. Increased nutrient loading may also lead to oxygen depletion when the water column is stratified. This gives a positive feed back to the phytoplankton in the water column with a complete break down of the system as a consequence.

2.2.1 Some Realizations of The Model

Figure 2.2 and 2.3 show realizations of the models described above with a specific set of parameter values. Figure 2.2 is deterministic, i.e. the noise term is set to zero; this is also called (see Tong (1990)) the skeleton of the stochastic model in Figure 2.3. Such plots allow us to examine the deterministic part of the model.

Figure 2.2 show the biomass level in the pelagic and the benthic zone as time

series. The same figure gives the time series of the nutrient level. From the figure we see that the system is stable in regime I with the nutrient input equal to 3. At $t = 10$ the input is increased to 6. The result is an increase in the phytoplankton biomass and a decrease in the benthic biomass. When this reaches the threshold value a dramatic increase in the phytoplankton level is seen and the benthic biomass disappear completely. Decreasing the nutrient load to 2 does not affect the benthic biomass level, while a further decrease to 1 results in an increase in the benthic biomass level and eventually a regime shift. With a further increase of loading to 3 the system return to the starting position. This kind of hysteresis, where we need to do more than returning to the original loading is expected in these kinds of ecosystems.

Figure 2.3 show a realization of a process like in Figure 2.2, but with noise added. This plot is included to give an example of how this would look with noise. It is seen that there are some unphysical inputs/outputs, with negative biomass and negative nutrient loading. This is due to the way the noise terms are included, but this problem could be fixed by transformation of data, e.g. by log-transforming the data. It is further noticed that the system end up in a "unhealthy" regime due to the stochastic input.
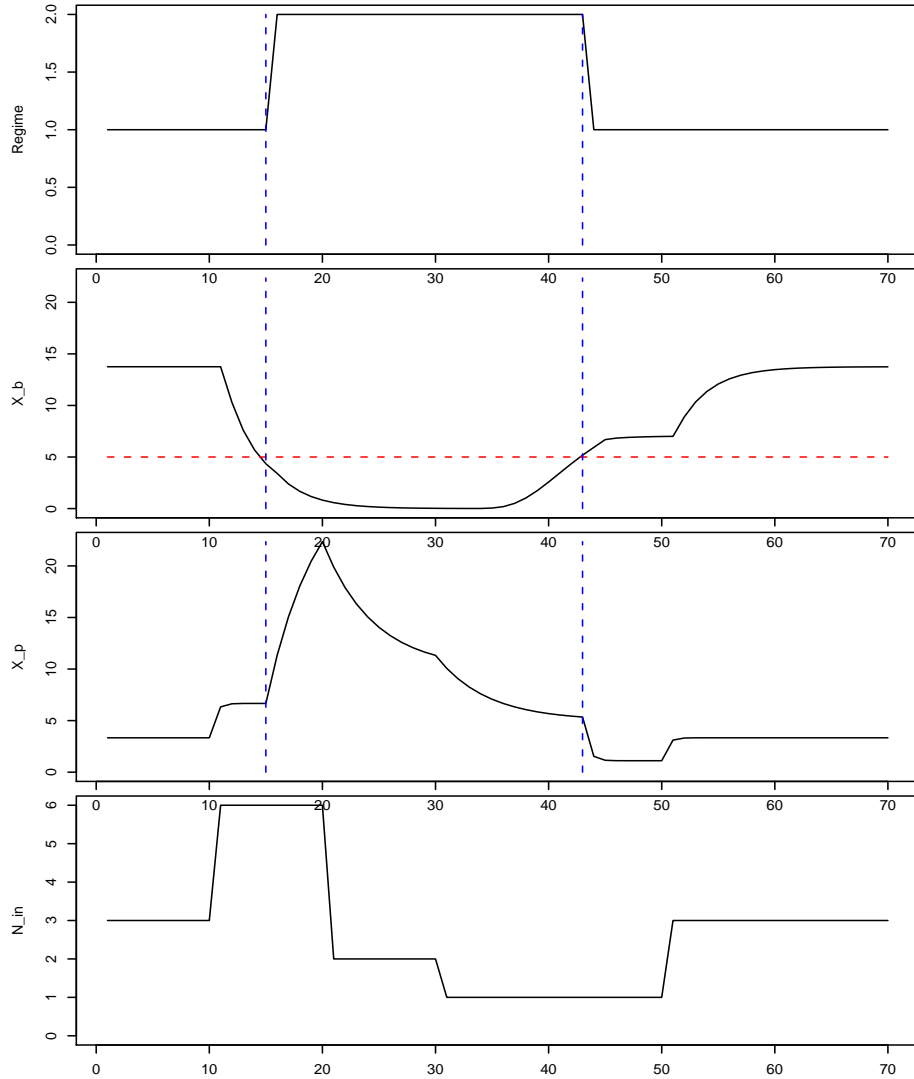
Figure 2.2: The model in Eq. (2.1) - (2.3) with $a_p^{(j)} = b_{p,b}^{(j)} = k^{(j)} = \tau_p^{(j)} = 1$, $b_b^{(j)} = 0.7$, $\epsilon_{p,t}^{(j)} = \epsilon_{b,t}^{(j)} = 0$, $r_p^{(j)} = 5$, $r_b = 5$ for $j \in \{1, 2\}$, $b_p^{(1)} = 0.1$, and $b_p^{(2)} = 0.8$. The plots show the regime which the model is in, the red line in the second row indicate the threshold, the bottom row show the load on the system.
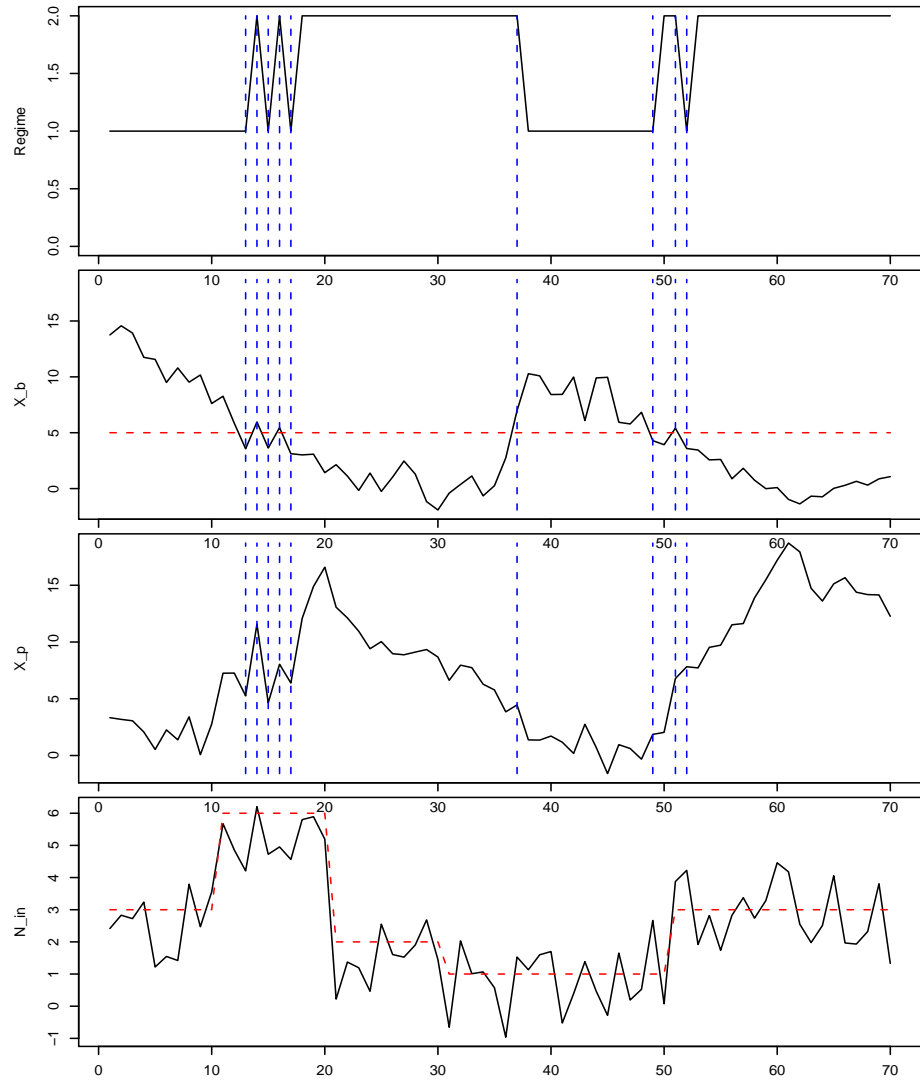
A Stochastic Model

Figure 2.3: Realization of the same model as in Figure 2.2, but with $\epsilon_{p,t}^{(j)}$ and $\epsilon_{b,t}^{(j)}$ iid. $N(0,1)$ distributed random variables and $N_{ex,t} = u_t + \epsilon_{N,t}$ where $\epsilon_{N,t}$ is $N(0,1)$ distributed random variables and u_t is deterministic. u_t is indicated with the red line in the bottom row.

2.3 A Smooth Threshold Set Up

A more general class of models than the SETAR-class is the class of Smooth Threshold "AR" (STAR) models. Replacing the hard threshold/"SETAR" term in (2.1) with a smooth threshold/"STAR" term give the model (in matrix notation)

$$
\begin{bmatrix} X_{p,t} \\ X_{b,t} \end{bmatrix} = N_{ex,t} \begin{bmatrix} a_p \\ 0 \end{bmatrix} + \begin{bmatrix} b_{p,t-1} & 0 \\ b_{p,b}f_{t-1} & b_b \end{bmatrix} \begin{bmatrix} X_{p,t-1} \\ X_{b,t-1} \end{bmatrix} + \begin{bmatrix} 0 \\ Kf_{t-1} \end{bmatrix}
$$
$$
+ \begin{bmatrix} \sigma_{1,1} & \sigma_{1,2} \\ \sigma_{2,1} & \sigma_{2,2} \end{bmatrix} \begin{bmatrix} \epsilon_{p,t} \\ \epsilon_{b,t} \end{bmatrix} \tag{2.5}
$$

or in a more compact notation

$$
\boldsymbol{X}_t = N_{ex,t}\boldsymbol{a} + B_t \boldsymbol{X}_{t-1} + \boldsymbol{k}_t + \Sigma \boldsymbol{\epsilon}_t \tag{2.6}
$$

The function $f_t = f(X_{p,t})$ is defined in the same way as in the previous sections, while the hard threshold from the SETAR-like model is replaced with the function

$$
b_{p,t} = (1 - \Phi(x_{b,t}, r_b, \tau_b^2))d + t_p \tag{2.7}
$$

This formulation means that $b_{p,t}$ changes from t_p to $t_p + d$ as X_b goes from $-\infty$ to ∞. In the limit $\sigma_b \to 0$, $\Phi(x_{b,t}, r_b, \tau_b^2)$ becomes the indicator function $I(x_{b,t} > r_b)$ and this model is the SETAR model presented in Section 2.2. This also means that r_b in (2.7) play the same role as the threshold parameter r_b for the SETAR model discussed above.

Figure 2.4 gives the time series plot for a STAR model with the same parameters as the SETAR model presented in Figure 2.2 and $\sigma_p = 1$. It is seen that the models behave similarly when the same pressure is imposed. The most significant difference between the two models is the shoulder in x_b; this is however not an asymptotic behavior.

Figure 2.5 shows the stationary points for the SETAR and the STAR models presented in Figure 2.2 and 2.4 as a function of the nutrient loading. The plots are constructed by finding the solution to the problem at $N_{ex} = 0$, then increasing the loading a little finding the solution here with the solution at $N_{ex} = 0$ as a starting guess and so on and so fourth until $N_{ex} = 6$. Then decreasing loading in the same way. Each stationary point is found by iteration until the number $\|\boldsymbol{x}_t - \boldsymbol{x}_{t-1}\|$ is small ($< 10^{-5}$) or the number of iterations reach a maximum number (50). A first observation from the two plots is that the models also in this case are quite similar. However one difference is that the SETAR process does not seem to converge for a range of small loadings.
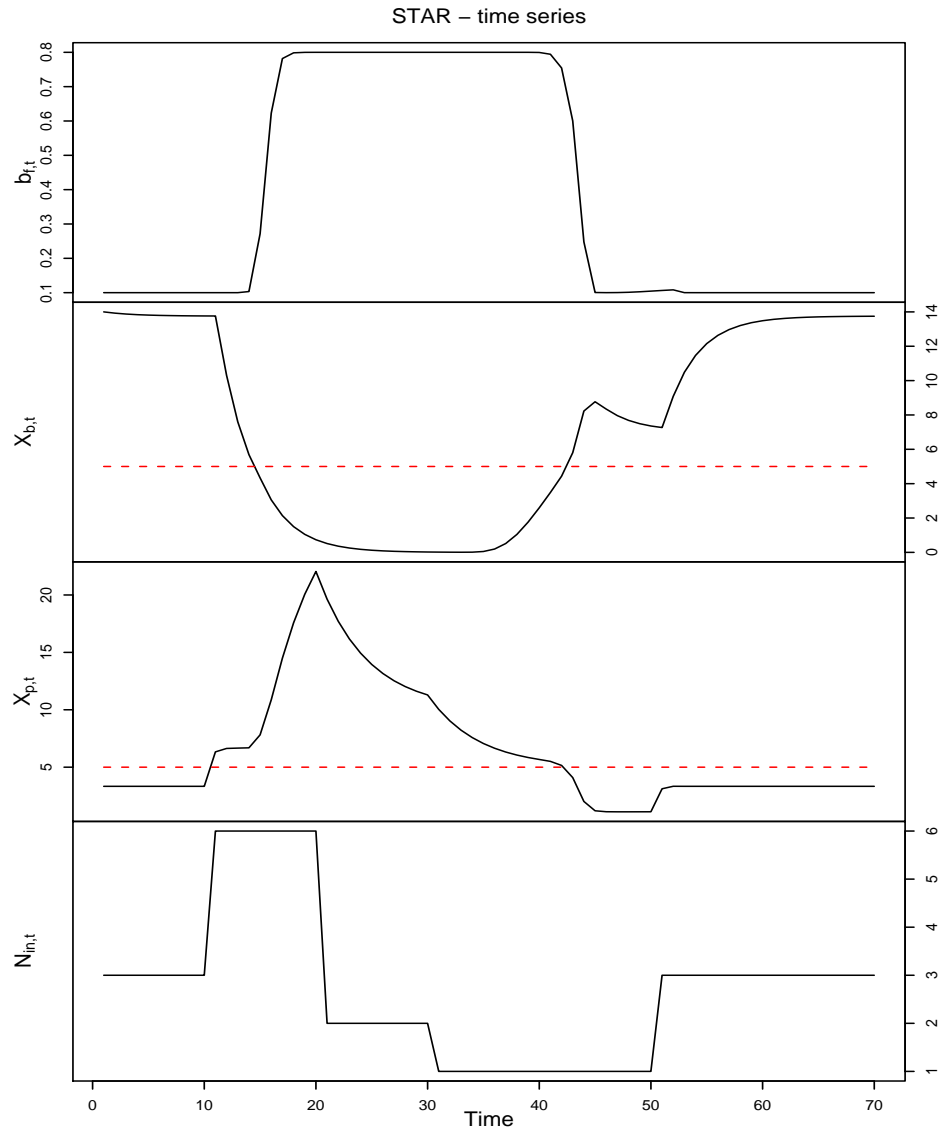
11

Figure 2.4: The model in Eq. (2.5) with $a_p = b_{p,b} = K = \tau_p = \tau_b = 1$, $b_b^{(j)} = 0.7$, $\epsilon_{p,t}^{(j)} = \epsilon_{b,t}^{(j)} = 0$, $r_b = r_p = 5$, $d = 0.7$, and $t_p = 0.1$. The plots show the regime which the model is in, the red line in the second row indicate the threshold, the bottom row show the load on the system.

This behavior might seem strange since we would expect systems to converge. Fortunately it is possible to analyze this behavior with standard analysis and algebra. To this end note that

$$f_t = f(x_p; r_p, r_p) = 1 - \Phi(x_{p,t}; 5, 1) \tag{2.8}$$

For the realization in Figure 2.5 it is seen that x_p is quite far (more $3r_p$) from r_p. It is therefore safe to set $f_t = 1$ in our analysis.

This gives a model that is linear in each of the two regimes defined by the threshold parameter r_b. The model in each of the regimes is therefore (with constant loading N_{ex})

$$\begin{bmatrix} x_{p,t} \\ x_{b,t} \end{bmatrix} = \begin{bmatrix} N_{ex}a_p \\ K \end{bmatrix} + \begin{bmatrix} b_p^{(j)} & 0 \\ b_{p,b} & b_b \end{bmatrix} \begin{bmatrix} x_{p,t-1} \\ x_{b,t-1} \end{bmatrix}$$

At the stationary points we must have $\boldsymbol{x}_t = \boldsymbol{x}_{t-1}$. Therefore we solve for stationary points, in each of the regimes and get the stationary points

$$\begin{bmatrix} x_p \\ x_b \end{bmatrix} = \begin{bmatrix} 1 - b_p^{(j)} & 0 \\ b_{p,b} & 1 - b_b \end{bmatrix}^{-1} \begin{bmatrix} N_{ex}a_p \\ K \end{bmatrix}$$

$$= \begin{bmatrix} \frac{1}{1-b_p^{(j)}} & 0 \\ \frac{b_{p,b}}{(1-b_p^{(j)})(1-b_b)} & \frac{1}{1-b_b} \end{bmatrix} \begin{bmatrix} N_{ex}a_p \\ K \end{bmatrix}$$

A necessary condition for this actually being a stationary point is that it is in the same regime as the model. If $x_b^{(j)}$ denotes the stationary point in regime j then a stationary point must satisfy

$$x_b^{(1)} > r_b \quad \vee \quad x_b^{(2)} < r_b \tag{2.9}$$

Now this conditions can be formulated in terms of conditions on the loading

$$N_{ex} > \left(r_b - \frac{K}{1-b_b} \right) \frac{(1-b_p^{(1)})(1-b_b)}{a_p b_{pb}} \tag{2.10}$$

or

$$N_{ex} < \left(r_b - \frac{K}{1-b_b} \right) \frac{(1-b_p^{(2)})(1-b_b)}{a_p b_{pb}} \tag{2.11}$$

plugging in the parameter values used for the simulation in Figure 2.5 we get

$$N_{ex} > \left(5 - \frac{1}{1-0.7} \right) \frac{(1-0.1)(1-0.7)}{1} = 0.45 \tag{2.12}$$

13

or

$$N_{ex} < \left(5 - \frac{1}{1 - 0.7}\right) \frac{(1 - 0.8)(1 - 0.7)}{1} = 0.1 \qquad (2.13)$$

These numbers are confirmed in Figure 2.6 where a zoom on the no converging region of the data is given. In summary; Figure 2.5 and 2.6 show that the process converge to a point in the other regimes. As the process approach this point the process change and converge to a point in the first regime and so on. Figure 2.6 and 2.7 show that these processes are not chaotic but that they form periodic signals. Note that for the analysis applied here it is important that x_p is far away from r_p. The non-stationary points are actually limit cycles as exemplified in Figure 2.7.

2.4 More Simulation Studies

Figure 2.8 shows empirical quantiles based on a simulation study with the model given in Figure 2.4, but with a noise term, i.e. $\Sigma = I$ and $\epsilon_{j,t} \sim N(0, 1)$. Further the input series have also been added noise. The figure shows how the uncertainty grow with time.

Figure 2.9 shows histogram for the parameters at time 70. These figures show that there is a splitting of the density function. I.e. there is a probability of being in "regime I" and a probability of being in "regime II", but the probability of being "between" these regimes is close to zero. E.g. the number of observed b_f in the interval $(0.2, 0.7)$ is 26 (giving a frequency of about 1%).

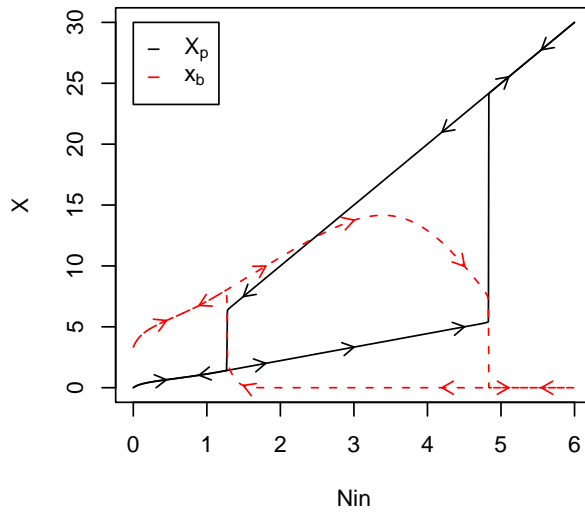## SETAR – stationary points
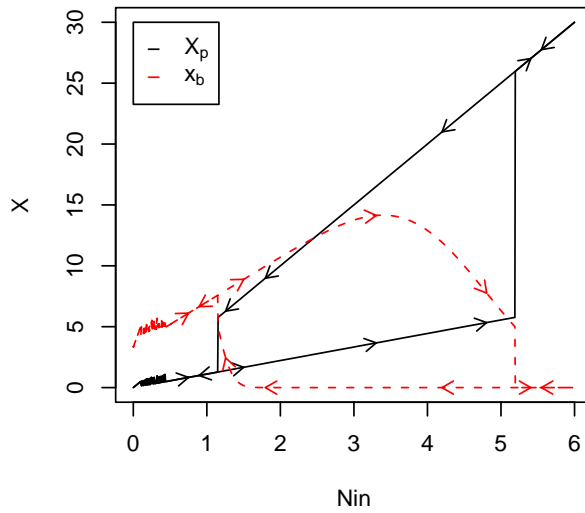
STAR – stationary points

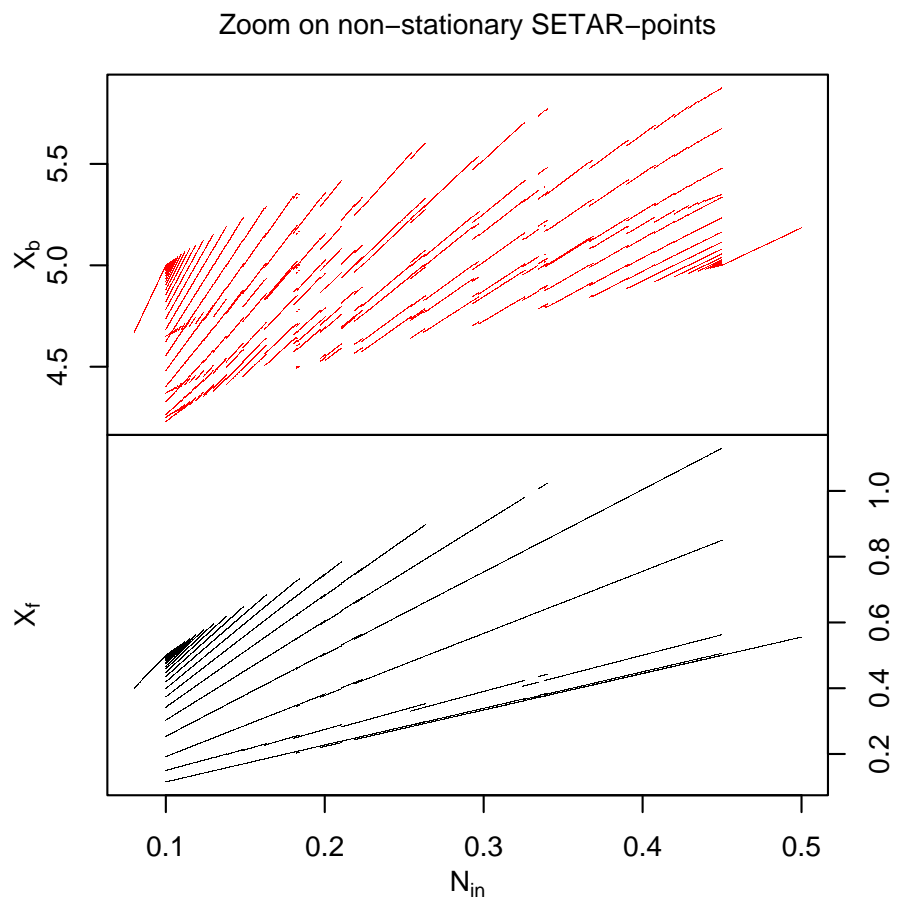Figure 2.5: Stationary points for the process in Figure 2.2 (top) and 2.4 (bottom) as a function of loading.

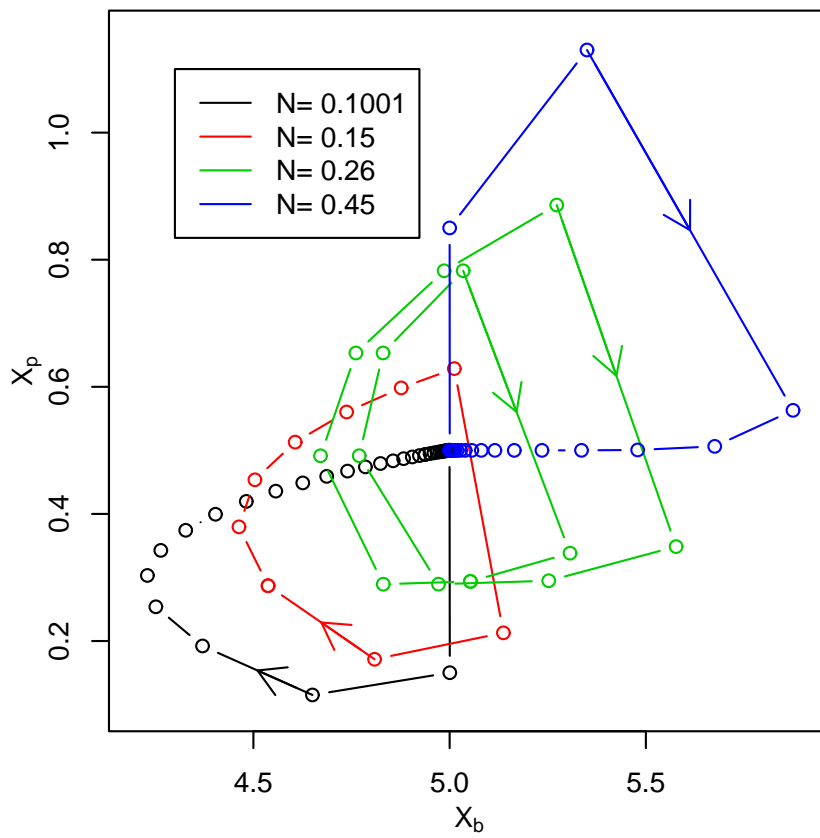Figure 2.6: Zoom on the non-stationary points of Figure 2.5.

Figure 2.7: Limit cycles for some of the non-stationary points given Figure 2.6.
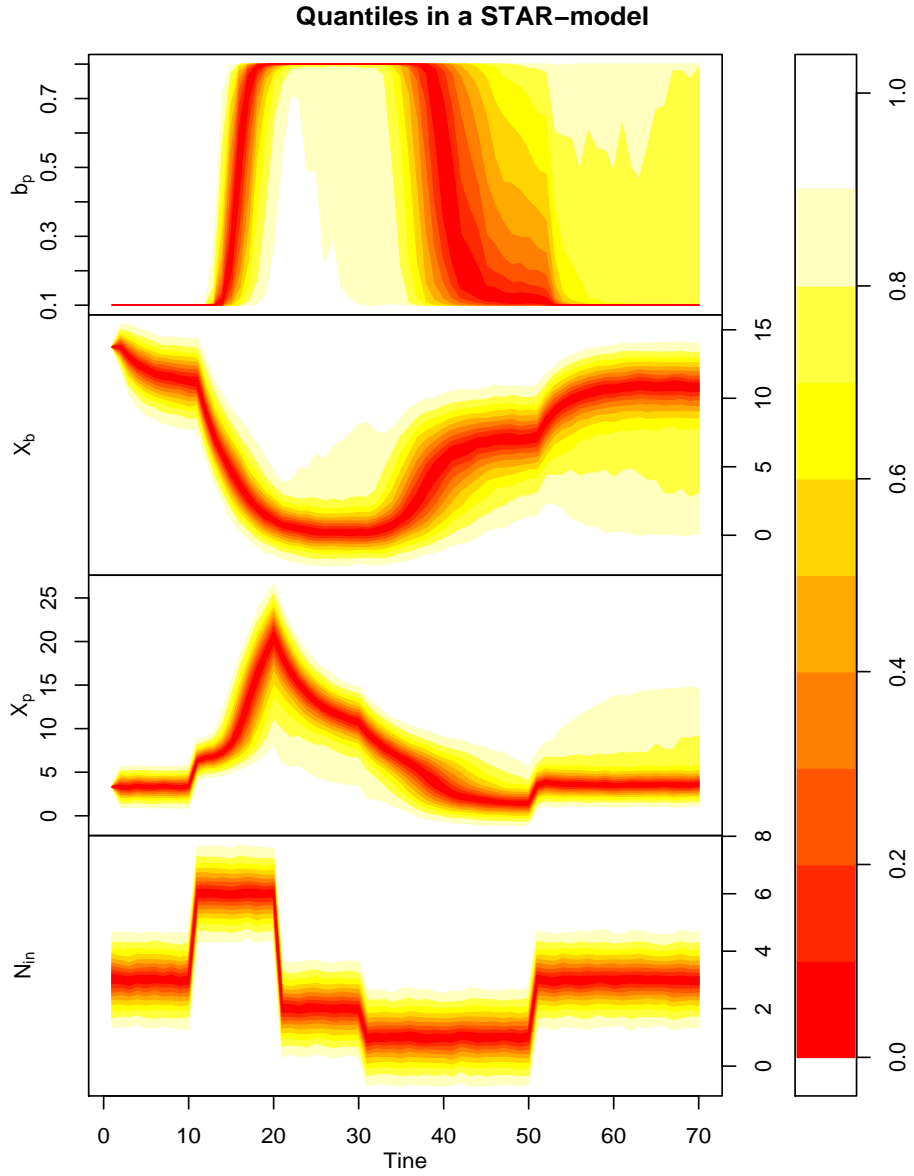
Figure 2.8: Empirical quantiles in a stochastic STAR model with $a_p = b_{p,b} = K = r_f = \tau_b = 1$, $b_b^{(j)} = 0.7$, $\epsilon_{p,t}^{(j)} = \epsilon_{b,t}^{(j)} \sim N(0,1)$, $r_b = r_p = 5$, $d = 0.7$, and $t_p = 0.1$. The nutrient input is given by $N_{ex,t} = N_t + u_t$ where N is a deterministic process given in Figure 2.4 and $u_t \sim N(0,1)$. The quantiles are based on 2000 time series.
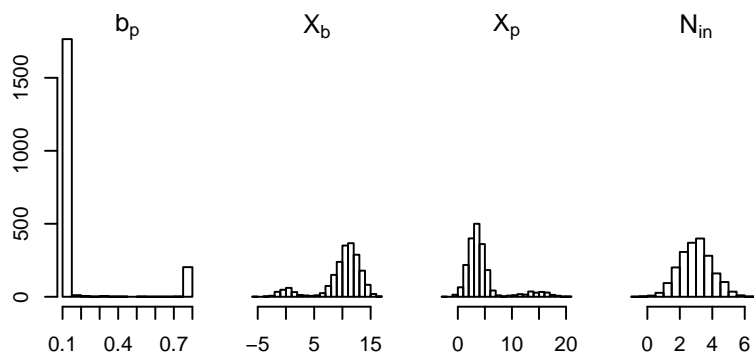
Figure 2.9: The figure show histograms of the data at time $t = 70$ used for the quantile plot in Figure 2.8.

Chapter 3

Including the Sediment

A more advanced model is now implemented. The idea is to capture the interactions in a more realistic way. This model contains a variable describing the nutrient content in the active part of the sediment and this is modeled as a state variable. The model is

$$
X_{p,t} = \underbrace{a_{ex}N_{ex,t}}_{Term1} + \underbrace{b_{p,t}N_{sed,t}}_{Term2a} \tag{3.1}
$$

$$
X_{b,t} = \underbrace{f_{sed,t}f_{light,t}b_{sl}(X_{b,t-1}+k)}_{Term3} + \underbrace{b_b X_{b,t-1}}_{Term4} \tag{3.2}
$$

$$
= (f_{sl,t}+b_b)X_{b,t-1} + kf_{sl,t} \tag{3.3}
$$

$$
N_{sed,t} = \underbrace{a_{NS}N_{sed,t-1}}_{Term5} + \underbrace{b_{p,sed}X_{p,t-1}}_{Term6} + \underbrace{(1-b_b-f_{sl,t})X_{b,t-1}}_{Term7} - \underbrace{b_{p,t}N_{sed,t}}_{Term2b} \tag{3.4}
$$

$$
\Downarrow
$$

$$
N_{sed,t} = \frac{1}{1+b_{p,t}}\left(a_{NS}N_{sed,t-1} + b_{p,sed}X_{p,t-1} + (1-b_b-f_{sl,t})X_{b,t-1}\right)
$$

The idea of this model is that the sediment works as a nutrient pool where nutrient from dead phytoplankton is stored until it returns to the water column or is permantly removed. The benthic vegetation uses the nutrient pool in the sediment to expand and dead vegetation will contribute to this nutrient pool. Note that $N_{sed,t}$ is not observable.

Each of the terms will be presented in the following.

Term 1:

This is a loading term, which determine what part of the nutrient loading $N_{ex,t}$ that is used locally. This fraction is a_{ex}. Note here that external loading of the system only enters the nutrient cycle of the system through the pelagic vegetation (phytoplankton).

Term 2 (a and b):

The terms describe how nutrients from the sediment pool are released to pelagic production. This process depends on the "regime" that the system is in. In the "healthy" regime $b_{p,t}$ should be small and in the "unhealthy" regime it should be large. This correspond to the situation described in earlier sections. $b_{p,t}$ is given by

$$b_{p,t} = (1 - \Phi(X_{b,t-1}, r_p, \tau_p^2))d + t_p \tag{3.5}$$

where Φ is the normal distribution function. d and t_p determine the intercept and range of $b_{p,t}$. $b_{p,t}$ gives the part of the nutrients from the sediment that goes into the pelagic vegetation. It is noticed that the nutrient in the sediment at time t is used rather than the nutrients at time $t - 1$. This is because the phytoplankton is assumed to die every winter and go into the sediment and then rise every year by use of the available nutrient. The term is subtracted in the expression for nutrient in the sediment.

Term 3:

The term describes how the benthic vegetation is influenced by the limiting factors, namely nutrients in the sediment and the light that is able to reach the benthic zone. These two limiting terms are given by

$$f_{sed,t} = \Phi(N_{sed,t-1}, r_{sed}, \tau_{sed}^2) \tag{3.6}$$
$$f_{light,t} = 1 - \Phi(X_{p,t-1}, r_{light}, \tau_{light}^2) \tag{3.7}$$

The product of these describes the growth potential under given conditions. This is multiplied by the level of benthic vegetation plus a constant term k. k can be conceived as the potential of new vegetation to be transported into the area from other locations. Mathematically k ensure that the steady state solution is different from zero. b_{sl} is a constant term and this should be chosen in such a way that the solution is stable. $b_b + b_{sl} < 1$ will ensure this, but due to the non-linearity of the expression it possible that this can be partly relaxed. This analysis is, however, not trivial.

Term 4:

The term describes how much of the benthic vegetation, which is carried over from one year to the next.

Term 5:

This is the fraction of avaliable nutrients in the sediment carried over from one year to the next. The fraction of nutrients not carried over will be permanently buried.

Term 6:

The term describes the part of the dead phytoplankton which stays in the system.

Term 7:

The term is the part of $X_{b,t}$ not carried over from one year to the next.

The equations given above is given without noise and this is also the way these will be analyzed in the next section.

3.1 Realizations

A realization of this model is given i Figure 3.1. The loadings in this figure is a series of estimated loading of the Danish waters, from Conley et al (in press).

The figure shows a break down of the system around 1960. The benthic vegetation disappears completely and the pelagic vegetation experiences a dramatic growth. This regime shift is also seen in the parameters in the right column of the figure. It is also worth to note that f_{sed} is not really active (with values between 0.94 and 1).

Figure 3.2 shows stationary points for the model in figure 3.1. The figure shows a hysteresis effect when nutrient loading is increased above approximately 4.5, when the system breaks down. A good indicator for the system seems to be b_p, since the shift in this parameter is very clear.

Figure 3.3 shows the same plot as Figure 3.2, but with a different set of parameter values. It is seen that there is also a hysteresis like transition as the loading is decreased from 6 to 0. It is quite clear that the model can display some very complicated behavior.
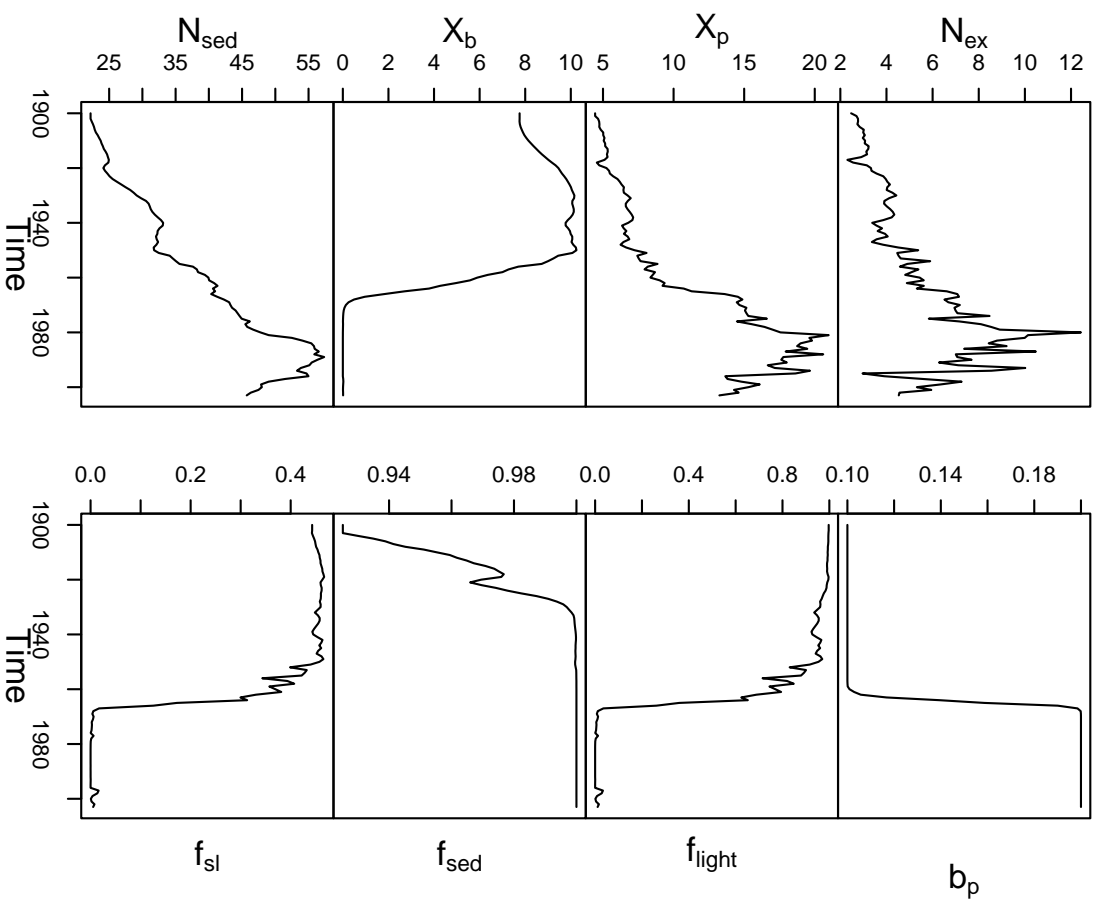
Figure 3.1: A realization of the model described in Eq. (3.1)-(3.4) with the parameters given in Table 3.1
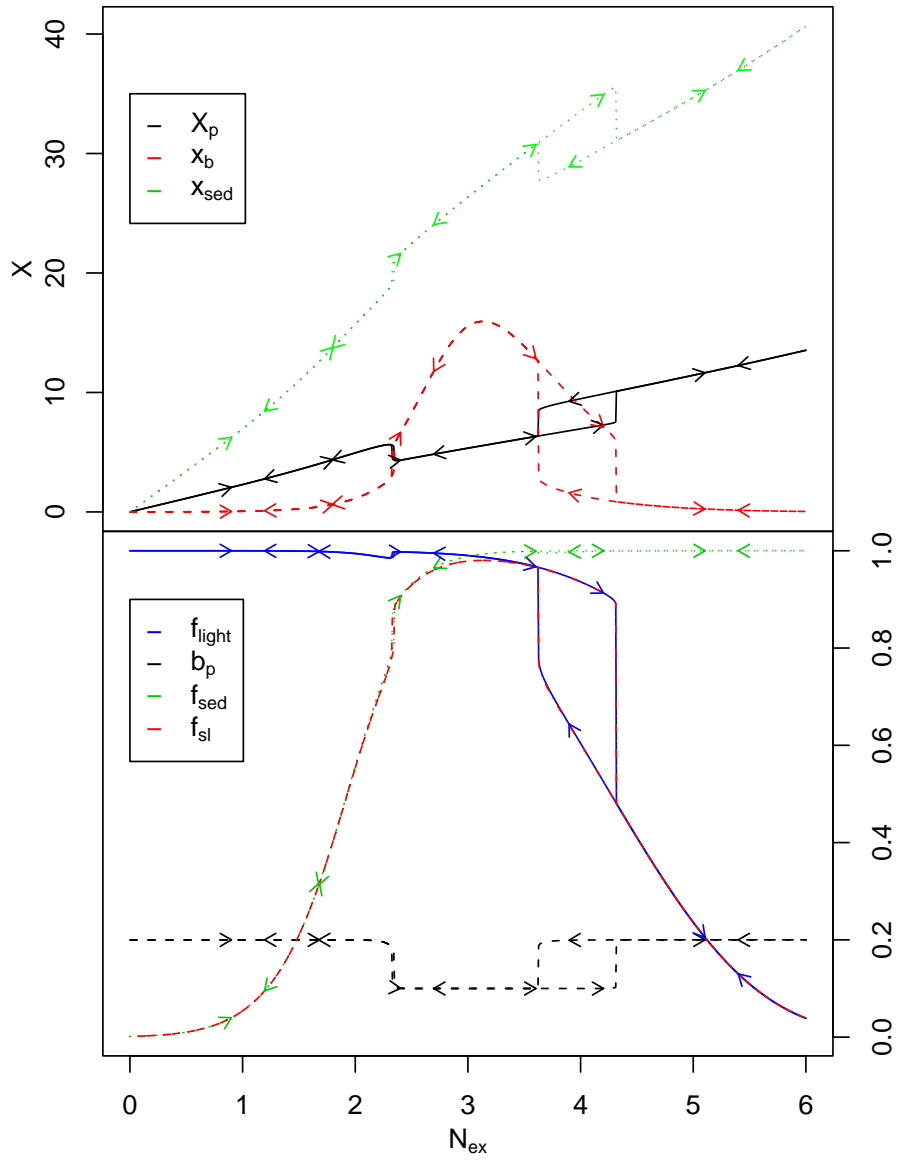
24

Figure 3.2: Stationary points of the model given in Eq. (3.1) - (3.4), for the parameter values in Table 3.1

Parameter	Fig 3.1 and 3.2	Fig 3.3
μ_p	4	4
μ_{light}	10	10
μ_{sed}	15	15
σ_p	1	1
σ_{light}	2	2
σ_{sed}	5	2
d	0.1	0.2
t_p	0.1	0.1
b_b	0.5	0.5
b_{sl}	0.48	0.48
$b_{p,sed}$	0.9	0.9
a_{NS}	0.9	0.9
a_{ex}	0.9	0.9
k	1	1.5

Table 3.1: Parameters for the mdels presented in Figure 3.1-3.3

3.2 Some Analytic Results

The model given above is very nonlinear and a complete analytical analysis is not possible. It is, however, possible to say something on the stability of the model or rather the requirements that have to be imposed on the parameters to ensure that the model is stationary. Such conclusions will only apply in some part of the space, or rather for some specific loadings.

To do this analysis the nonlinear functions are simply assumed to be constant and the steady state solution under this assumption is calculated. The system equation is now written as a multivariate time series model, i.e. we get

$$
\begin{bmatrix} 1 & 0 & -b_p \\ 0 & 1-(b_b+f_{sl})B & 0 \\ -b_{p,sed} & (b_b+f_{sl}-1)B & 1+b_p-a_{NS}B \end{bmatrix} \begin{bmatrix} X_{p,t} \\ X_{b,t} \\ N_{sed,t} \end{bmatrix} = \begin{bmatrix} a_{ex}N_{ex} \\ f_{sl}k \\ 0 \end{bmatrix} \tag{3.8}
$$

where B is the back shift operator ($Bx_t = x_{t-1}$). Following Jenkins and Alavi (1981) this system could be written in a compact form as

$$
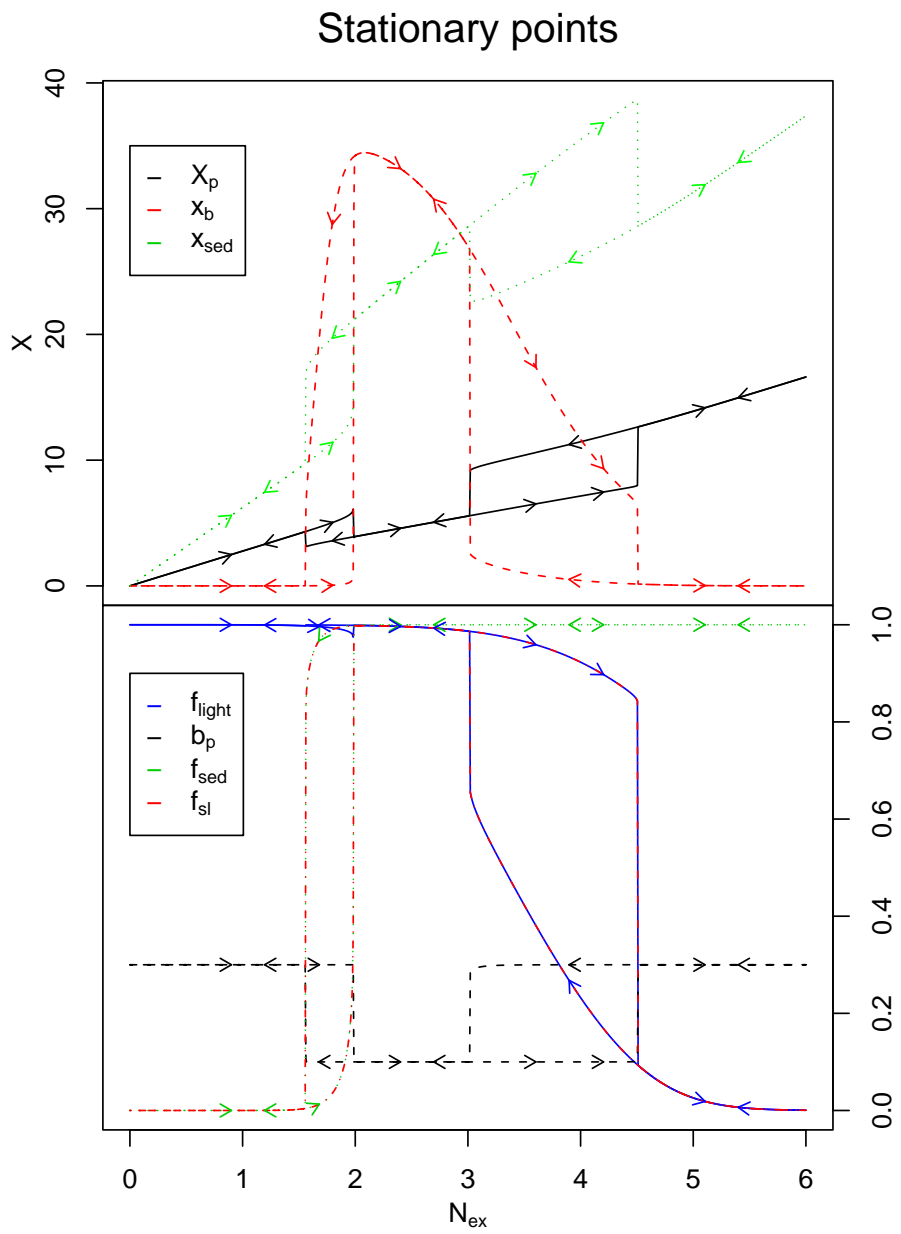\Phi(B)\boldsymbol{X}_t = \boldsymbol{a}_t \tag{3.9}
$$

26

Figure 3.3: Stationary points of the model in Eq. (3.1) - (3.4) for the parameter values in Table 3.1

Such a system will be stable if the roots of $det(\Phi(z^{-1}))$ lie inside the unit circle. The determinant of $\Phi(z^{-1})$ is

$$det(\Phi(z^{-1})) = \frac{(z - f_{sl} - b_b)(z(1 + b_p) - a_{NS} - b_{p,sed}b_p)}{z^2} \qquad (3.10)$$

The roots of this equation is given directly as

$$z = \begin{cases} f_{sl} + b_b \\ \frac{b_{p,sed}b_p + a_{NS}}{1 + b_p} \end{cases} \qquad (3.11)$$

If this had been a linear system, then the requirements would be

$$f_{sl} + b_b < 1 \quad \text{and} \quad \frac{b_{p,sed}b_p + a_{NS}}{1 + b_p} < 1 \qquad (3.12)$$

The parameters in the model are to be thought of as fractions of the components. E.g. b_p describes the part of the nutrient in the sediment that move to the watercolumn.

Chapter 4

Discussions and Conclusions

We have presented two different models for the interaction between benthic and pelagic production. These have been analyzed in a framework of multivariate time series analysis. The models are nonlinear, the nonlinearities are imposed in such a way that we can simulate regime shift imposed by increased nutrient loadings. The models are quite simple in the sense that the models only contain two or three state variables. The models are, however, able to display very complicated behavior like thresholds, hysteresis and multiple hysteresis effect. Such behavior are important, because it is the hypothesis that biological system can contain hysteresis and threshold effect.

For the two-state model we presented a hard threshold model and a smooth threshold model. We consider the smooth threshold approach advantageous to the hard threshold approach since this is more general in the sense that it contains the hard threshold model as a special example. In addition the smooth threshold model, have smooth transitions (even if these can be very fast) as would be expected in nature.

In the presented models, there is one parameter that can control the hysteresis span. It is therefore straight forward to control this span.

The presented models have not been quantitatively compared to data. It is of course an important issue to go from the parameter calibration presented here to parameter estimation. The ability to do this is of course limited by the data series available.

Even though the models presented here are quite simple, there is still large degree of freedom within the model structure and the non-linearity of the models can lead to very different behavior of models that are seemingly close. It is therefore important to have tools that in a simple way can distinguish between models. This could e.g. be the stability or sensitivity of a model. These features of the mod-

els should preferably be described in one single number in such a way that it is possible to compare models in a quantitatively way.

Bibliography

Carpenter S. R., Ludwig D. and Brock W. A. (1999) *Management of Eutrophication for Lakes Subject to Potentially Irreversible Changes.* Ecological Applications, 1999, 9(3), pp. 751-771

Carpenter S. R. (2005). *Eutrophication of Aquatic Ecosystems: Bistability and Soil Phosohorus.* PNAS, July 2005, vol. 102, no. 29, pp. 10002-10005

Conley, D.J., J. Carstensen, G. Ærtebjerg, P.B. Christensen, T. Dalsgaard, J.L.S. Hansen & A. Josefson (in press): *Long-term changes and impacts of hypoxia in Danish coastal waters.* Ecological Applications.

Giusti E. & Marsili-Libelli S. (2004) *Modelling the Interaction between Nutrients and the Submerged Vegetation in the Ortobetello Lagoon* Ecological Modelling 184, pp. 141-161.

Jenkins G. M. and Alavi A. (1981) *Some Aspects of Modeling and Forecasting Multivariate Time Series.* Journal of Time Series Analysis, Vol.2 Issue. 1, p. 1-47.

Ludwig D., Carpenter S. R. and Brock W. A. (2003) *Optimal Phosphorus Loading for a Potentially Eutrophic Lake.* Ecological Applications, 13(4), pp. 1135-1152

Schindler D. W. (2006) *Recent advances in the understanding and management of eutrophication.* Limnology and Oceanography, 51 (1, part 3), pp. 356-363

Scheffer M., Szabó S.,van Nes E. H., Rinaldi S., Kautsky N., Norberg J., Roijackers R. M. M. and Franken R. J. M. (2003) *Floating Plant Dominance as a Stable State.* PNAS, vol. 100, no.7, pp. 4040-4045

Tong H. (1990) *Non-linear Time Series - A Dynamical System Approach.* Oxford Science University Press